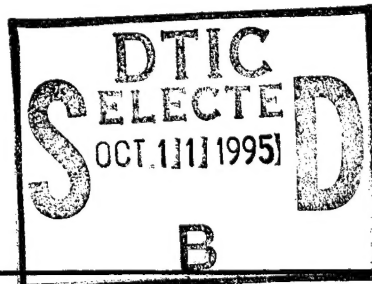


# REPORT DOCUMENTATION PAGE

Form Approved  
OMB No. 0704-0188

Public reporting burden for this collection of information is estimated to average 1 hour per response, including the time for reviewing instructions, searching existing data sources, gathering and maintaining the data needed, and completing and reviewing the collection of information. Send comments regarding this burden estimate or any other aspect of this collection of information, including suggestions for reducing this burden, to Washington Headquarters Services, Directorate for Information Operations and Reports, 1215 Jefferson Davis Highway, Suite 1204, Arlington, VA 22202-4302, and to the Office of Management and Budget, Paperwork Reduction Project (0704-0188), Washington, DC 20503.

1. AGENCY USE ONLY (Leave blank)		2. REPORT DATE 8/10/95	3. REPORT TYPE AND DATES COVERED FINAL: 9/1/93--6/30/95	
4. TITLE AND SUBTITLE  "A Combined X-ray Scattering and Molecular Modeling Study of Manufacturing Processing of Polymers and Composites"			5. FUNDING NUMBERS  DAAH04-93-G-0347	
6. AUTHOR(S)  Prof. Peggy Cebe				
7. PERFORMING ORGANIZATION NAME(S) AND ADDRESS(ES)  Massachusetts Institute of Technology 77 Mass. Avenue, Cambridge MA 02139			8. PERFORMING ORGANIZATION REPORT NUMBER	
9. SPONSORING / MONITORING AGENCY NAME(S) AND ADDRESS(ES)  U.S. Army Research Office P.O. Box 12211 Research Triangle Park, NC 27709-2211			10. SPONSORING / MONITORING AGENCY REPORT NUMBER	
11. SUPPLEMENTARY NOTES The views, opinions and/or findings contained in this report are those of the author(s) and should not be construed as an official Department of the Army position, policy, or decision, unless so designated by other documentation.				
12a. DISTRIBUTION / AVAILABILITY STATEMENT  Approved for public release; distribution unlimited.			12b. DISTRIBUTION CODE	
13. ABSTRACT (Maximum 200 words)  Measurement of the coefficient of thermal expansion(CTE) of the crystalline lattice of two semicrystalline thermoplastic polyimides are reported. NEW-TPI and LARC-CPI polyimides were studied using high temperature Wide angle X-ray scattering from 25C up to 325C. Systematic shifts in the a-, and b-axis lattice parameters were seen. No c-axis expansion was detected.				
14. SUBJECT TERMS  polyimides, thermal expansion, X-ray scattering			15. NUMBER OF PAGES 35	
			16. PRICE CODE	
17. SECURITY CLASSIFICATION OF REPORT UNCLASSIFIED	18. SECURITY CLASSIFICATION OF THIS PAGE UNCLASSIFIED	19. SECURITY CLASSIFICATION OF ABSTRACT UNCLASSIFIED	20. LIMITATION OF ABSTRACT UL	



19951005 051

DTIC QUALITY INSPECTED 5

**A COMBINED X-RAY SCATTERING AND MOLECULAR MODELING STUDY OF  
MANUFACTURING PROCESSING OF POLYMERS AND COMPOSITES**

**INTERIM REPORT  
SEPTEMBER 1, 1993 - JUNE 30, 1995**

For the portion of work performed at:  
Department of Materials Science and Engineering  
Massachusetts Institute of Technology  
Cambridge, MA 02139

Contract Monitor: Dr. Robert Reeber

Professor Peggy Cebe  
Department of Physics and Astronomy  
Tufts University

August 7, 1995

**THE U.S. ARMY RESEARCH OFFICE  
AASERT CONTRACT No. DAAH04-93-G-0347**

The views, opinions, and/or findings contained in this report are those of the author and should not be construed as an official department of the Army position, policy, or decision, unless so designated by other documentation.

## TABLE OF CONTENTS

	<u>Page</u>
List of Tables .....	3
List of Figures .....	4
<b>1. HIGHLIGHTS OF DAAH04-93-G-0347 .....</b>	<b>5</b>
1.1 Research Accomplishments .....	5
1.2 Budget .....	5
1.3 Students Supported .....	5
1.4 Publications and Presentations .....	6
1.5 Collaborations Established .....	6
<b>2. RESEARCH ACCOMPLISHMENTS .....</b>	<b>7</b>
3.1 Thermal Expansion .....	7
3.2 Experimental Section .....	8
3.3 LARC-CPI.....	9
3.4 NEW-TPI.....	12
3.5 Coefficient of Thermal Expansion .....	14
<b>3. REFERENCES .....</b>	<b>17</b>
<b>4. TABLES .....</b>	<b>19</b>
<b>5. FIGURES .....</b>	<b>23</b>

<b>Accession For</b>	
NTIS GRA&I	<input checked="" type="checkbox"/>
DTIC TAB	<input type="checkbox"/>
Unannounced	<input type="checkbox"/>
Justification	
By	
Distribution/	
Availability Codes	
Dist	Avail and/or Special
A-1	

## List of Tables

Page

- Table 1 Comparison of properties of NEW-TPI and LARC-CPI.
- Table 2 D-spacings for the (110) and (200) planes and lattice parameters a, b, and c as a function of temperature for NEW-TPI.
- Table 3 D-spacings for the (111) and (200) planes and lattice parameters a and b as a function of temperature for LARC-CPI.
- Table 4 Lattice parameter c as a function of temperature for LARC-CPI.

## List of Figures

Page

- Figure 1      Chemical structures for one repeat unit of NEW-TPI and LARC-CPI.
- Figure 2      WAXS intensity vs.  $2\theta$  for cold crystallized films of NEW-TPI at 25°C (solid line) and 275°C (dashed line).
- Figure 3      Lattice parameters a (squares) and b (circles) vs. temperature for NEW-TPI.
- Figure 4      WAXS intensity vs.  $2\theta$  for NMP treated films of NEW-TPI at 25°C (solid line) and 325°C (dashed line).
- Figure 5      NEW-TPI: a.) Peak index number of the 00l reflections, n, vs.  $2\sin\theta/\lambda$  at 25°C. b.) Lattice parameter c vs. temperature.
- Figure 6      WAXS intensity vs.  $2\theta$  for cold crystallized films of LARC-CPI at 25°C (solid line) and 275°C (dashed line).
- Figure 7      WAXS intensity vs.  $2\theta$  for NMP treated films of LARC-CPI at 25°C (solid line) and 300°C (dashed line).
- Figure 8      Peak index number of the 00l reflections, n, vs.  $2\sin\theta/\lambda$  for LARC-CPI at 25°C.
- Figure 9      Lattice parameters a(squares) and b (circles) vs. temperature for LARC-CPI.
- Figure 10     Unit cell volume vs. temperature: a.) NEW-TPI; b.) LARC-CPI.

## 1. HIGHLIGHTS OF DAAH04-93-G-0317 (9/93-6/95)

### 1.1. Research Accomplishments

1. The commercial software package, Cerius<sup>TM</sup>, was used in molecular modeling of the crystal structure of LARC-CPI thermoplastic polyimide. Unit cell lattice parameters were determined for this polymer for the first time.
2. Cerius<sup>TM</sup> and Polygraf<sup>TM</sup> were used to determine the energy minimized repeat unit length for LARC-CPI.
3. Cerius<sup>TM</sup> and Polygraf<sup>TM</sup> were used to determine the chain conformation of a series of liquid crystalline polycarbonates prepared by Dr. Heidi Schreuder-Gibson's group at the Army Natick Laboratory.
4. Wide angle X-ray scattering studies were performed on fibers of dimethyl-substituted stilbene liquid crystalline polycarbonates.
5. Wide angle X-ray scattering studies were performed on film stacks of LARC-CPI and NEW-TPI thermoplastic polyimides.
6. Thermal expansion coefficients for the crystalline unit cell of LARC-CPI and NEW-TPI were determined for the first time.
7. Angle resolved X-ray photoelectron spectroscopy was performed on the surface of NEW-TPI and a strong ordering peak was characterized as belonging to an ordered diamine.

### 1.2 Budget

Amount Spent 9/1/93 - 6/30/95	\$ 26,719.74
Time Period of Expenditure	22 months
Total Budget	\$ 99,791
Total Period of Grant	36 months

### 1.3 Students Supported (months of support) and Present Status

Mark Brillhart(6)	M. S., MIT 6/94
Ingchie Kwan(5)	S. B., MIT, expected 6/96
Paul Kang(4)	S. B., MIT, expected 6/96
Christine Tsau(5)	S. B., MIT, expected 6/98

### 1.4 Publications and Presentations

1. Mark V. Brillhart and Peggy Cebe. "Thermal Expansion of the Crystal Lattice in Novel Thermoplastic Polyimides." *J. Polym. Sci., Polym. Phys. Ed.*, **33**, 927 (1995).
2. Yao-Yi Cheng, Mark Brillhart, Peggy Cebe, Heidi Schreuder-Gibson, Aaron Bluhm, and Walter Yeomans. "Wide-angle X-ray Scattering Study of Liquid Crystalline Polycarbonates Based on a-Methyl Stilbene Mesogen and Methylene-Containing Flexible Spacer," *Mol. Cryst./Liq. Cryst.*, in press 1995.
3. Yao-Yi Cheng, Mark Brillhart, Peggy Cebe, and Malcolm Capel. "Small Angle X-ray Scattering, Thermal and Mechanical Analysis of Poly(butylene terephthalate)/Polycarbonate Blends." *Macromolecules*, in preparation for submission 9/95.
4. July 1995, "Real-Time Small-Angle X-ray Scattering from Blends," American Crystallographic Association Conference, Montreal, Canada.
5. September 1995, "Crystallization of Monotropic Liquid Crystalline Polycarbonates Based on a-Methyl Stilbene Mesogen," North American Thermal Analysis Society Conference, San Francisco, CA.
6. December 1995, "Real-Time Small-Angle X-ray Scattering from Blends." 1995 International Chemical Congress of Pacific Basin Societies, Honolulu, HA.

### 1.5 Collaborations Established

**Dr. Malcolm Capel** is beam line manager of the X12B beam at the Brookhaven National Synchrotron Light Source and a faculty member of the *Brookhaven Biology Department*. Dr. Capel is co-author on research performed at NSLS and funded under this contract.

**Dr. Heidi Schreuder-Gibson** is a synthetic polymer chemist at the *U.S. Army Natick Research, Development and Engineering Center*. We are collaborating on a project in thermotropic liquid crystalline polymers which have application potential in Soldier Protection. I am using real-time x-ray scattering to characterize phase transformations in LCPs synthesized by Dr. Schreuder-Gibson.

### 3.0 RESEARCH ACCOMPLISHMENTS

#### 3.1 Thermal Expansion

Measurements of the coefficient of thermal expansion (CTE) of the crystalline lattice of two semicrystalline thermoplastic polyimides are reported. NEW-TPI and LARC-CPI polyimides were studied using elevated temperature wide angle X-ray scattering (WAXS) from 25°C to 325°C. To examine possible shifts in the c-axis, a novel approach developed in our lab [1,2] was used to create highly oriented samples. Films were treated in 1-methyl-2-pyrrolidinone (NMP) at the reflux temperature, washed and then dried under constraint. The films treated in this manner were highly oriented, with c-axes preferentially aligned along the film normal. The advantage of this orientation is that it allows numerous reflections of type (00l) to be examined for temperature shifts of the c-axis using reflection mode WAXS. No systematic shift of the c-axis lattice parameter as a function of temperature was observed in either NEW-TPI or LARC-CPI. The c-axis thermal expansion is concluded to be smaller than  $8 \times 10^{-6}/^{\circ}\text{C}$  for LARC-CPI, and for NEW-TPI may be weakly negative. From WAXS of unoriented films, systematic shifts in the a and b lattice parameters were deduced as a function of temperature. The linear CTEs relating these unit cell parameters at temperature T to their values at 0°C are:

<u>NEW-TPI</u>	<u>LARC-CPI</u>
$a = 7.82 (1 + 93 \times 10^{-6}T)$	$a = 8.06 (1 + 117 \times 10^{-6}T)$
$b = 6.36 (1 + 60 \times 10^{-6}T)$	$b = 6.12 (1 + 75 \times 10^{-6}T)$

The novel class of high performance semicrystalline polyimides (PIs) has been the subject of recent studies by our group [1-8] and others [9-34]. Regulus<sup>TM</sup> NEW-TPI (Mitsui Toatsu Chemical Co.) [1-6,14,20-30] and LARC-CPI (NASA Langley Research Center) [2,7-25] are two promising polyimides which have potential applications as wire and cable insulation, composite matrices, and high temperature films. The chemical structures of these polyimides are shown in Figure 1[1,14,17]. NEW-TPI monomer unit contains the pyromellitic dianhydride (PMDA), while LARC-CPI contains the benzophenone tetracarboxylic dianhydride (BTDA). As a result of



incorporation of phenyl-ether and phenyl-ketone linkages into the diamine component, the molecular mobility is increased allowing crystallization to occur from the melt [9-15]. Both materials can be processed by standard thermoforming techniques such as injection molding and extrusion of pellets or film [27,28] and can be drawn into oriented films [5,7]. A comparison of properties of NEW-TPI and LARC-CPI is shown in Table 1. The glass transition temperatures are 250°C (TPI) [25] and 222°C (CPI) [14], while the crystal melting temperatures are 388°C (TPI) [25] and 350°C (CPI) [14]. Both polyimides reach an ultimate degree of crystallinity around 0.30-0.40 [4,7].

Because the formation temperature from the melt is several hundred degrees above room temperature, thermal contraction properties of PIs during processing will be important. Applications involving adhesion to substrates, or formation of composite structures, will likewise be affected by the coefficient of thermal expansion. The bulk linear CTEs of several polyimides have been reported by Numata, et al. [35-38]. PI films were cured either on or off a substrate, and relationship of bulk linear CTE to chemical structure was investigated [35-37]. The CTE was temperature dependent, so an average value from 50-250°C was reported. Bent structures generally had higher CTEs. For PIs containing BTDA, bulk linear CTE ranged from  $3-5 \times 10^{-5}/K$ , while PIs containing PMDA, which is a more rigid group, had lower CTE ranging from  $1-2 \times 10^{-5}/K$  [35-38].

On this basis, we expect bulk linear CTE to be smaller in NEW-TPI than in LARC-CPI, and this has been observed [6]. In this report, we investigate the crystal lattice expansion properties of these novel semicrystalline polyimides determined from elevated temperature WAXS.

### 3.2. Experimental Section

Elevated temperature isothermal WAXS experiments were performed on a Rigaku RU200 system in  $\theta/2\theta$  reflection mode. The generator was operated at 50KV and 200mA, and produced Cu  $K_{\alpha}$  radiation at  $\lambda=1.54\text{\AA}$ . 1 degree diffraction and scatter slits were used with both 0.15 and 0.30 degree receiving slits. Receiving slits were selected to optimize the intensity of the diffraction pattern peaks.  $2\theta$  was continuously varied at a rate of 0.1 degree per minute in the range from 3 to 40 degrees at a step scan interval of 0.02 degrees.

Scans were made on both cold crystallized and NMP treated stacks of films of NEW-TPI and LARC-CPI. Amorphous films of NEW-TPI

(Regulus<sup>TM</sup>) were provided by Mr. Yasunori Sugita of Mitsui Toatsu Chemical Company. LARC-CPI samples were provided in the form of partially imidized solvent cast films and were obtained from Dr. Terry St. Clair of the NASA Langley Research Center.

Semicrystalline films of NEW-TPI were heated to 300°C and held for 1 hour. The temperature was then rapidly increased to 340°C and the films were immediately cooled to room temperature at a rate of -20°C/minute. Semicrystalline samples of LARC-CPI were prepared by a similar cold crystallization process. The specimens were heated to 170°C and held for 1 hour. The temperature was then ramped to 190°C and held for another hour, to complete the imidization process. This was carried out in two steps to eliminate the foaming that can occur during this chemical reaction if too fast a heating rate is used. The sample was then heated to 300°C and held for 1 hour, then cooled to room temperature at a rate of -20°C/minute.

Films of both NEW-TPI and LARC-CPI were subjected to an NMP treatment that was developed in our lab to create highly oriented films [1,2]. Films of both materials were placed in an NMP bath at the reflux temperature, 204°C, under Argon protection gas. The NMP does not dissolve the films (no weight loss was observed after treatment) but acts as a plasticizer allowing crystallization to occur as a result of the increased molecular mobility. As-received NEW-TPI films were heated in NMP for 4 hrs. Fully imidized LARC-CPI samples were heated in NMP for 18 hrs. After NMP treatment, samples were washed in distilled water at room temperature for 4 hrs to remove any residual NMP. No NMP was detected by FTIR analysis of the washed films. The samples were then placed between filter paper, and clamped between two perforated ceramic plates. This clamping process constrained the films by holding them flat during drying in a vacuum oven at 106°C overnight.

### 3.3 NEW-TPI

Figure 2 shows WAXS intensity vs.  $2\theta$  for cold crystallized NEW-TPI films at 25°C (solid line) and 275°C (dashed line) over the angular range from 13 to 30 degrees. The noise level in the scan is indicated by the vertical marker. The Miller indices,  $hkl$ , for the five crystalline reflections shown in Figure 2 were determined from the crystal structure of NEW-TPI presented by Okuyama, et al. [21,22]. Miller indices are marked at the room temperature peak positions in Figure 2. Table 2 lists the  $d$ -spacing vs. temperature for the

(110) and (200) planes. Error estimates in this table, and all other tables and figures, are based on an assumed uncertainty in angle  $\theta$  of 0.05 degrees. There is a systematic shift to larger d-spacing as temperature increases for all reflections of the type (hk0). In this scan, there is one reflection, (112), with non-zero  $l$  index. The temperature shift of this peak is very small. Because the (112) peak occurs as a shoulder on the much stronger (110) reflection, we did not attempt to analyze its temperature shift.

From the (200) reflection the lattice parameter  $a$  was determined as a function of temperature by solving:

$$1/(d_{hkl})^2 = (h/a)^2 + (k/b)^2 + (l/c)^2 = (2 \sin \theta_{hkl} / \lambda)^2 \quad (1)$$

where  $d_{hkl}$  is the d-spacing of the planes with Miller indices,  $hkl$ ;  $a, b, c$  are the lattice parameters for the orthorhombic unit cell;  $\theta_{hkl}$  is the half scattering angle; and  $\lambda$  is the X-ray wavelength. There was no reflection of the type (0k0) in the WAXS scan of NEW-TPI. However, with knowledge of lattice parameter  $a$ , lattice parameter  $b$  could be found from (110) and (210). Lattice parameter  $b$  has a larger relative error than lattice parameter  $a$ . Lattice parameters  $a$  and  $b$  determined from equation (1) are listed in Table 2 and displayed in Figure 3. There is a systematic change in both lattice parameters with temperature. The lines drawn through the data in Figure 3 represent the lines of best fit and were used to determine the CTE which will be reported in Section 3.3. We assume that the crystal structure remains orthorhombic throughout the temperature range. No signature of a crystal lattice transformation was observed in either thermal analysis or in small angle X-ray scattering studies at elevated temperature [6].

We developed a method to produce highly oriented films by recrystallization in NMP [1,2], following the observation by Wang, et al. [32] that a (usually) amorphous polyimide, LARC-TPI, could be crystallized in NMP. The procedure for NMP film treatment and drying is described in the experimental section, and results in films having  $c$ -axes oriented preferentially along the film normal. The geometric constraints of the hot hutch mounted on the Rigaku diffractometer are such that the films must be examined in  $\theta/2\theta$  reflection mode. Our NMP treated films with  $c$ -axes aligned along the film normal possess the correct orientation for WAXS studies in  $\theta/2\theta$  reflection mode. Standard methods for producing oriented films, for example

by zone annealing, hot drawing or rolling, result in orientation with the fiber axis lying in the plane of the film, and hence can not be used for the present studies.

Figure 4 shows the scan of NMP treated NEW-TPI with peaks indexed according to the crystal structure determined by Okuyama, et al. [21,22]. The solid line represents data at 25°C, while the dashed line indicates changes in the scan which occur at 325°C. Numerous reflections of the type (00*l*) can be seen in Figure 4, along with two small peaks having either *h* or *k* non-zero. The only systematic changes with temperature occurred in the (200) and (210) peaks, as indicated by the dashed lines in Figure 4 which show how these reflections have shifted by the time the temperature has reached 325°C.

In a study of PEEK thermal expansion, Blundell and D'Mello [39] used a single (00*l*) reflection to determine the lattice parameter *c*. These researchers found some variation in the lattice parameter *c* when different (00*l*) reflections were chosen. Here, our novel solvent exposure processing results in *c*-axes aligned along the film normal. This results in a large number of (00*l*) reflections which can be examined in  $\theta/2\theta$  reflection mode, and analyzed for a consistent value of *c*. The *c*-axis repeat distance, *d*, was found from the slope of:

$$n = d (2 \sin\theta/\lambda) \quad (2)$$

where *n* is the peak index, and  $\theta$  is the half scattering angle. Figure 5a shows peak index, *n*, vs.  $2\sin\theta/\lambda$  for the eight 00*l* reflections at room temperature. The slope gives a *c*-axis value of 25.3Å, which is slightly larger than the *c*-axis repeat distance, 25.11Å, found by Okuyama [21,22]. The slope of *n* vs.  $2\sin\theta/\lambda$  was evaluated at each temperature to determine the *c*-axis shift. These results are shown in the last column of Table 2 and illustrated in Figure 5b. There is perhaps a slight trend for a decrease in the *c*-axis as a function of increasing temperature, but within the error bars ( $\pm 0.02\text{\AA}$ ), the *c*-axis did not change systematically with temperature. The error bars on these data were established from consideration of the  $\chi^2$ , the sum of the squares of the deviations of *c*-axis data from the line of best fit. At each temperature, the best fit line was determined. The error bar limits shown in Figure 5b represent the extreme values of *c* that would result in a 50% increase of  $\chi^2$ . Deviations of this size could easily be determined to be "poor fits" by visual inspection. Within the resolution of this instrument, the *c*-axis of the crystal lattice of NEW-TPI

remains approximately constant over the temperature range from 25°C to 325°C. The changes in *a* and *b* lattice parameters are significant and well outside the error limits on these quantities.

The coherence length of crystals, *t*, in a direction perpendicular to a set of lattice planes of Miller index *h,k,l* can be determined approximately from the Scherrer equation [40]:

$$t = K \lambda / (\beta_{hkl} \cos \theta_{hkl}) \quad (3)$$

where  $\beta_{hkl}$  is the broadening due to crystal size, and *K* is the Scherrer constant which is assumed here to equal 0.89. Effects of lattice strain are not included here. If the peaks are further assumed to have Gaussian lineshape, then the broadening due to crystallite size is found from the measured peak full width at half maximum, *B*, and the instrumental broadening, *b*, according to:

$$\beta^2 = B^2 - b^2 \quad (4)$$

This evaluation was made for the room temperature scans. Using the (200) peak we find a coherence length in the *a*\* direction of 110Å. The coherence length in the *a*\* direction is 14.0 times the length of the unit cell lattice parameter *a*. Averaging  $\beta$  from the (004), (005), (006), (007), (009), and (0010) peaks we find a coherence length in the *c*\* direction of 108Å. This indicates the NEW-TPI crystal is about 4 monomer repeat units thick.

### 3.4 LARC-CPI

Figure 6 shows WAXS intensity vs.  $2\theta$  for cold crystallized LARC-CPI films at 25°C and 275°C over the angular range from 15 to 30 degrees. Again, the noise level in the scans is shown by the vertical markers. Miller indices for the three crystalline reflections shown in Figure 6 were determined from our prior study of the crystal lattice of LARC-CPI [7,8] and mark the room temperature positions of the peaks. All of the peaks are broad and there is a systematic shift to larger *d*-spacing as temperature increases for all three reflections. Table 3 lists the *d*-spacing vs. temperature for the (111) and (200) planes which are the most intense contributors to the reflections shown in Figure 6 [8]. The lattice parameter *a* could be determined directly; lattice parameter *b* required knowledge of the *c*-axis for its evaluation.

Figure 7 shows WAXS intensity vs.  $2\theta$  for NMP treated LARC-CPI films at 25°C (solid line) and 300°C (dashed line). The intense sharp peak at 28.44° is from the Si calibration standard. The majority of the peaks in the WAXS scan of NMP treated LARC-CPI are of the type (00 $l$ ). None of the (00 $l$ ) peaks shifted systematically as the temperature increased. Only two peaks showed significant shift as a function of temperature: the one attributed to the overlap of (110), (111), (112), (008) and the small peak attributed to (200).

Figure 8 shows the peak index vs.  $2\sin\theta/\lambda$  for the eight (00 $l$ ) reflections at room temperature. The  $c$ -axis at each temperature was evaluated from the slope, and results are listed in Table 4. The  $c$ -axis of LARC-CPI is erratic and shows no trend as a function of temperature. Within our instrument resolution the  $c$ -axis of LARC-CPI is invariant with temperature changes over the interval from 25°C to 300°C. On the other hand, when lattice parameter  $a$  was evaluated using the small (200) peak shown in Figure 7, a systematic variation with temperature was observed. Since the (200) peak intensity was quite weak in the NMP treated samples, evaluation of lattice parameter  $a$  was made from the unoriented WAXS pattern of Figure 6

Lattice parameters  $a$  and  $b$  were determined, respectively, from (200) and (111)  $d$ -spacings in Table 3 by solving equation (1). Because the  $c$ -axis showed no systematic variation over the temperature interval, its average value over the interval (37.6Å) was chosen for use in the evaluation of the parameter  $b$  from (111). Results for lattice parameters  $a$  and  $b$  are listed in the last columns of Table 3 and displayed in Figure 9 as functions of temperature. The variation of lattice parameter  $a$  with temperature is substantial. Lattice parameter  $b$  has a larger relative error than lattice parameter  $a$  but still shows a positive thermal expansion. The lines through the data are the lines of best fit, and were used to determine the CTE.

The Scherrer equation [40] (see equation 3 above) was used to estimate the coherence length of LARC-CPI crystals at room temperature. From (200) peak broadening we find a coherence length in the  $a^*$  direction of 107Å, or 13 times the length of the lattice parameter  $a$ . Using  $\beta$  averaged from (003), (004), (007), (0010), and (0013) we find a coherence length in the  $c^*$  direction of 77Å, which is about two times the monomer repeat distance.

### 3.5 Coefficient of Thermal Expansion

The temperature dependence of the lattice parameters obtained from WAXS allows us to evaluate the linear coefficient of thermal expansion (CTE) of the crystalline portions of the material. A parameter,  $p$ , at elevated temperature,  $T$ , is related to its value  $p(0)$  at  $0^\circ\text{C}$  according to the relationship:

$$p(T) = p(0) [1 + \alpha_p T] \quad (5)$$

where  $\alpha_p$  is the linear CTE of parameter  $p$ . Thus the slope of the linear fit of the data is the product of the  $0^\circ\text{C}$  value of the parameter and  $\alpha_p$ .  $\alpha_a$  and  $\alpha_b$  were determined from equation (5) for both materials. Summarizing the results of the thermal expansion of the crystal lattice for these polyimides, we find the following relationship between the lattice parameters at elevated temperature,  $T$  (in degrees Centigrade) and their values at  $0^\circ\text{C}$ :

<u>NEW-TPI</u>	<u>LARC-CPI</u>
$a = 7.82 (1 + 93 \times 10^{-6}T)$	$a = 8.06 (1 + 117 \times 10^{-6}T)$
$b = 6.36 (1 + 60 \times 10^{-6}T)$	$b = 6.12 (1 + 75 \times 10^{-6}T)$

In both polyimides, the  $a$ -axis expansion was greater than that of the  $b$ -axis. The results for LARC-CPI  $a$ -axis expansion were determined from the (200) peak of unoriented film (Figure 6). When the small (200) peak of the NMP treated sample (Figure 7) was used to obtain  $\alpha_a$ , we find  $\alpha_a = 110 \times 10^{-6}/^\circ\text{C}$ , which agrees very well with the  $\alpha_a$  shown above.

Neither NEW-TPI nor LARC-CPI  $c$ -axis lattice parameters exhibited unambiguous changes with temperature. Within the resolution of our instrument, we can only conclude that the  $c$ -axis expansion for LARC-CPI is smaller than  $10 \times 10^{-6}/^\circ\text{C}$ . For NEW-TPI the  $c$ -axis expansion might be weakly negative. The  $c$ -axes expansions are much smaller than either  $a$ - or  $b$ -axes expansions in both LARC-CPI and NEW-TPI. Thus, both materials are very anisotropic in their unit cell expansion characteristics. The same result was seen in another high performance thermoplastic polymer, PEEK, in which Blundell and D'Mello report no detectable expansion of the  $c$ -axis [39]. In another study of PEEK, Choy, et al. report  $c$ -axis expansion to be negative [41].

Ward and coworkers have reported negative axial thermal expansions for highly drawn films of poly(vinylidene fluoride) [42] and polypropylene [43].



They attribute negative expansion to shrinkage stresses that become relaxed at high temperature. Choy and Nakafuku found negative axial expansions for drawn polyoxymethylene [44]. They suggest that negative expansion relates to torsional and bending motions of the polymer chains.

On the other hand, undrawn polymers with flexible backbone bonds and low energetic barriers to rotation, can have much larger CTE in the c-axis direction. Our prior results on poly(butylene terephthalate), PBT, showed a c-axis expansion of  $213 \times 10^{-6}/^{\circ}\text{C}$ , which was comparable to the expansions in the a and b directions of the triclinic unit cell [45]. PBT contains a crumpled tetramethylene sequence that can expand to trans conformation over a low energy barrier. Polymers such as the novel polyimides studied here possess stiff backbone bonds that are highly resistant to rotation, leading to very low CTEs along the molecular chain axis. Expansion in directions perpendicular to the chain can occur more easily. Expansion in the a and b directions are resisted by relatively weak Van der Waals forces, and are energetically more favorable. The much greater expansion along a indicates the intermolecular forces are weaker in this direction than in the direction of b.

Since the a and b lattice parameters show a linear CTE over the temperature range studied, while the c lattice parameter is assumed invariant with temperature, there will be a linear volumetric expansion of the entire unit cell. Retaining only terms linear in the temperature, the volume expansion of the unit cell may be written as:

$$V(T) = V(0) [1 + \alpha_v T] \quad (6)$$

where  $\alpha_v$  is given in this approximation by:

$$\alpha_v = \sum_i \alpha_i = \alpha_a + \alpha_b + \alpha_c \quad (7)$$

Figure 10 a,b shows the maximum estimate for the unit cell volume, V, as a function of temperature for NEW-TPI and LARC-CPI, respectively. The volume coefficients of thermal expansion of the unit cell can be written according to equation (4) as:

$$\begin{array}{c} \text{NEW-TPI} \\ V \leq 1258 (1 + 153 \times 10^{-6}T) \end{array}$$

$$\begin{array}{c} \text{LARC-CPI} \\ V \leq 1855 (1 + 192 \times 10^{-6}T) \end{array}$$



For the two thermoplastic polyimides, NEW-TPI and LARC-CPI, we find that crystalline unit cell thermal expansion occurs predominantly along the a and b directions of the cell. A novel film preparation method allowed us to examine many orders of (00l) reflection. There was no expansion of the unit cell in the direction of the c-axis, within the resolution of our instrument. LARC-CPI has a larger crystal volume expansion coefficient than NEW-TPI. This indicates that LARC-CPI crystals will contract relatively more after melt processing than NEW-TPI.

### 3. REFERENCES

1. J. Friler and P. Cebe. *Polym. Eng. Sci.*, 33(10), 588 (1993).
2. J. B. Friler, M. S. Thesis (Massachusetts Institute of Technology, 1991).
3. P. P. Huo and P. Cebe. *Polymer*, 34(4), 696 (1993).
4. P. P. Huo, J. Friler and P. Cebe. *Polymer*, 34(21), 4387 (1994).
5. Y. Aihara and P. Cebe. *Polym. Eng. Sci.*, 34(16), 1275 (1994).
6. S. Lu, P. Cebe, and M. Capel. *J. Appl. Polym. Sci.*, in review (1994).
7. J. B. Teverovsky, D. C. Rich, Y. Aihara, and P. Cebe. *J. Appl. Polym. Sci.*, 54, 497 (1994).
8. M. V. Brillhart, P. Nagakar, and P. Cebe. *Polymer*, in review (1994).
9. P. M. Hergenrother. *Polym. J.*, 19(1), 73 (1987).
10. P. M. Hergenrother, N. T. Wakelyn and S. J. Havens. *J. Polym. Sci., Polym. Chem.*, 25, 1093 (1987).
11. P. M. Hergenrother and S. J. Havens. *J. Polym. Sci., Polym. Chem.*, 27, 1161 (1989).
12. P. M. Hergenrother and S. J. Havens. *SAMPE J.*, 24(4), 13 (1988).
13. P. M. Hergenrother and S. J. Havens. *Polyimides: Material, Chemistry, and Characterization*, Elsevier, Amsterdam, 453(1989).
14. P. Hergenrother, SPE Conference on High Temperature Polymers and Their Uses, Cleveland, OH, October 2-4, 1989.
15. D. Wilson, H. D. Stenzenberger, and P. M. Hergenrother. *Polyimides*, Chapman & Hall, New York (1990).
16. J. T. Muellerleile and G. Wilkes. *American Chemical Society, Polym. Preprints*, 31(2), 637 (1990).
17. J. T. Muellerleile and G. Wilkes. *Polym. Comm.*, 32(6), 176 (1991).
18. J. T. Muellerleile, B. G. Risch, D. K. Brandom, and G. Wilkes. *American Chemical Society, Polym. Preprints*, 33(1), 409 (1992).
19. J. T. Muellerleile, B. G. Risch, D. E. Rodrigues and G. Wilkes. *Polymer*, 34(4), 789 (1993).
20. M. Ohta, *Netsukokajushi*, 7, 199 (1989).
21. K. Okuyama, H. Sakaitani, and H. Arikawa. *Macromol.*, 25, 7261 (1992).
22. H. Sakaitani, K. Okuyama, and H. Arikawa, *Polym. Preprints Japan*, 40(1-4), 478 (1991).
23. S. Yuasa, M. Truji, and T. Takahashi, *Polym. Preprints Japan*, 40(1-4), 491 (1991).

24. T. H. Hou and R. M. Reddy, *SAMPE Quarterly*, January 1991, p. 38.
25. Technical data sheet/A00, NEW-TPI, Mistui-Toatsu Chemical Co., Tokyo, Japan.
26. T. Hirade, Y. Hama, T. Sasuga, and T. Seguchi, *Polymer*, 32(14), 2499 (1991).
27. K. Blizzard, R. Haghighat, R. Lusignea, and J. Connell. *SPE Antec XXXVIII*, 2253 (1992).
28. K. Blizzard and R. Haghighat. *Polym. Eng. Sci.*, in press (1993).
29. B. B. Sauer and B. S. Hsiao. *Polymer*, 34, 3315 (1993).
30. B. S. Hsiao, B. B. Sauer, and A. Biswas. *J. Polym. Sci., Polym. Phys. Ed.*, 32, 737 (1994).
31. T. L. St. Clair and A. K. St. Clair. *J. Polym. Sci., Polym. Chem. Ed.*, 15(6), 1529 (1977).
32. J. Wang, A. T. DiBenedetto, J. F. Johnson, S. J. Huang, and J. L. Cercena. *Polymer*, 30(4), 718 (1989).
33. T. L. St. Clair, H. D. Burks, N. T. Wakelyn, and T. H. Hou. *Amer. Chem. Soc., Polym. Preprints*, 28(1), 90 (1987).
34. T. L. St. Clair, M. K. Gerber, and C. R. Gautreaux. *Amer. Chem. Soc. Polym. Mat. Sci. Eng.*, 60, 183 (1989).
35. S. Numata, S. Oohara, J. Imaizumi, and N. Kinjo. *Polym. J.*, 17(8), 981 (1985).
36. S. Numata, S. Oohara, K. Fugisaki, J. Imaizumi, and N. Kinjo. *J. Appl. Polym. Sci.*, 31, 101 (1986).
37. S. Numata, K. Fugisaki and N. Kinjo. *Polymer*, 28(12), 2282 (1987).
38. S. Numata and T. Miwa. *Polymer*, 30, 1170 (1989).
39. D. J. Blundell and J. D'Mello. *Polymer*, 32(2), 304 (1991).
40. B. E. Warren, *X-ray Diffraction*, Addison-Wesley Pub. Co., Reading, MA, 251-254 (1969).
41. C. L. Choy, W. P. Leung, and C. Nakafuku. *J. Polym. Sci., Polym. Phys. Ed.*, 28, 1965 (1990).
42. S. J. Nanayakkara, G. A. Orchard, G. R. Davies, and I. M. Ward. *J. Polym. Sci., Polym. Phys. Ed.*, 25, 1113 (1987).
43. S. A. Jawad. G. A. Orchard and I. M. Ward. *Polymer*, 27(8), 1201 (1986).
44. C. L. Choy and C. Nakafuku. *J. Polym. Sci., Polym. Phys. Ed.*, 26, 921 (1988).
45. P. P. Huo, P. Cebe, and M. Capel. *J. Polym. Sci., Polym. Phys. Ed.*, 30, 1459 (1992).

## 4. Tables

Table 1

Comparison of properties of NEW-TPI and LARC-CPI.

Property	NEW-TPI	LARC-CPI
Glass Transition, °C	250°C [25]	222°C [14]
Melting Point, °C	388°C [25]	350°C [14]
Ultimate Crystallinity	0.30 [4]	0.40 [7]
Dielectric Constant (25°C, 1MHz)	3.2 [3]	3.1 [14]
Young's Modulus, GPa (25°C, 10Hz)	3.1 [2]	3.0 [7]
Crystal Density, g/cm <sup>3</sup>	1.47 [21]	1.51 [5]
Amorphous Density, g/cm <sup>3</sup>	1.33 [25]	1.335 [5]
Lattice Parameters (25°C):		
a-axis (Å)	7.89[21], 7.85 <sup>a</sup>	8.07 <sup>a</sup>
b-axis (Å)	6.29[21], 6.37 <sup>a</sup>	6.13 <sup>a</sup>
c-axis (Å)	25.11[21], 25.31 <sup>a</sup>	37.6 <sup>a,b</sup>

<sup>a</sup> Reported in this work

<sup>b</sup> Average value over the temperature interval

Table 2

D-spacings for the (110) and (200) planes and lattice parameters a, b, and c as a function of temperature for NEW-TPI.

Temp. (°C)	d <sub>110</sub> (Å)	d <sub>200</sub> (Å)	a (Å)	b (Å)	c (Å)
25	4.95±.015‡	3.92±.015‡	7.85±.015‡	6.37±.035‡	25.31±.02‡
50	4.95	3.93	7.86	6.37	25.34
75	4.96	3.94	7.88	6.38	25.32
100	4.97	3.95	7.89	6.39	25.31
125	4.98	3.96	7.91	6.40	25.30
150	4.99	3.97	7.93	6.42	----
175	4.99	3.97	7.93	6.42	25.33
200	5.01	3.98	7.97	6.44	----
225	5.01	3.99	7.97	6.44	25.29
250	5.02	4.00	7.99	6.45	25.27
275	5.04	4.01	8.03	6.47	25.27
300	5.04	4.03	8.05	6.47	----
325	5.05	4.03	8.07	6.48	25.27

---- Not tested at this temperature

‡ Error limits apply to all column entries

Table 3

D-spacings for the (111) and (200) planes and lattice parameters a and b as a function of temperature for LARC-CPI.

Temp. (°C)	d <sub>111</sub> (Å)	d <sub>200</sub> (Å)	a (Å)	b (Å)
20	4.84±.035‡	4.03±.015‡	8.07±.015‡	6.135±.035‡
52	4.86	4.06	8.12	6.14
77	4.87	4.07	8.15	6.15
102	4.88	4.08	8.16	6.17
127	4.89	4.09	8.18	6.185
150	4.90	4.10	8.20	6.195
176	4.90	4.11	8.23	6.19
200	4.91	4.12	8.23	6.20
226	4.94	4.14	8.28	6.23
251	4.94	4.15	8.29	6.24
276	4.96	4.17	8.33	6.25

‡ Error limits apply to all column entries

Table 4

Lattice parameter  $c$  as a function of temperature for LARC-CPI.

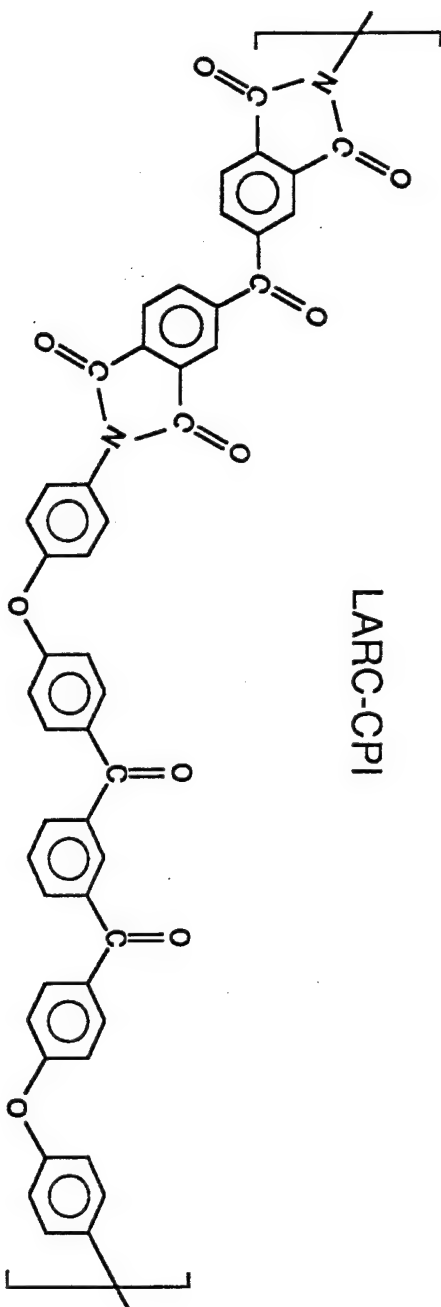
Temperature (°C)	$c$ (Å)
25	$37.50 \pm .02^\ddagger$
50	37.65
75	37.58
100	37.64
125	37.61
150	37.67
175	37.66
200	37.66
215	37.61
230	37.60
250	37.56
275	37.62
300	37.60

$^\ddagger$  Error limits apply to all column entries

## 5. Figure Captions

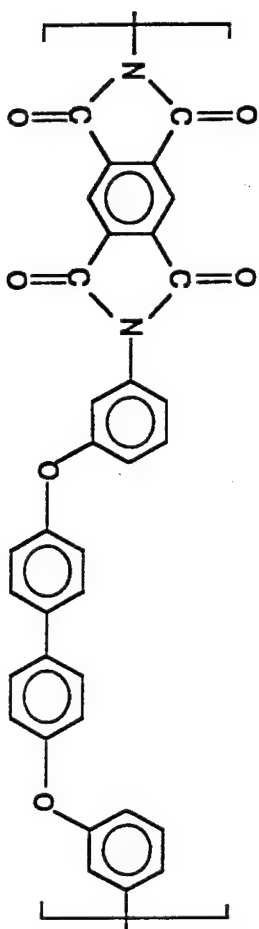
- Figure 1      Chemical structures for one repeat unit of NEW-TPI and LARC-CPI.
- Figure 2      WAXS intensity vs.  $2\theta$  for cold crystallized films of NEW-TPI at 25°C (solid line) and 275°C (dashed line).
- Figure 3      Lattice parameters a (squares) and b (circles) vs. temperature for NEW-TPI.
- Figure 4      WAXS intensity vs.  $2\theta$  for NMP treated films of NEW-TPI at 25°C (solid line) and 325°C (dashed line).
- Figure 5      NEW-TPI: a.) Peak index number of the 00l reflections, n, vs.  $2\sin\theta/\lambda$  at 25°C. b.) Lattice parameter c vs. temperature.
- Figure 6      WAXS intensity vs.  $2\theta$  for cold crystallized films of LARC-CPI at 25°C (solid line) and 275°C (dashed line).
- Figure 7      WAXS intensity vs.  $2\theta$  for NMP treated films of LARC-CPI at 25°C (solid line) and 300°C (dashed line).
- Figure 8      Peak index number of the 00l reflections, n, vs.  $2\sin\theta/\lambda$  for LARC-CPI at 25°C.
- Figure 9      Lattice parameters a(squares) and b (circles) vs. temperature for LARC-CPI.
- Figure 10     Unit cell volume vs. temperature: a.) NEW-TPI; b.) LARC-CPI.

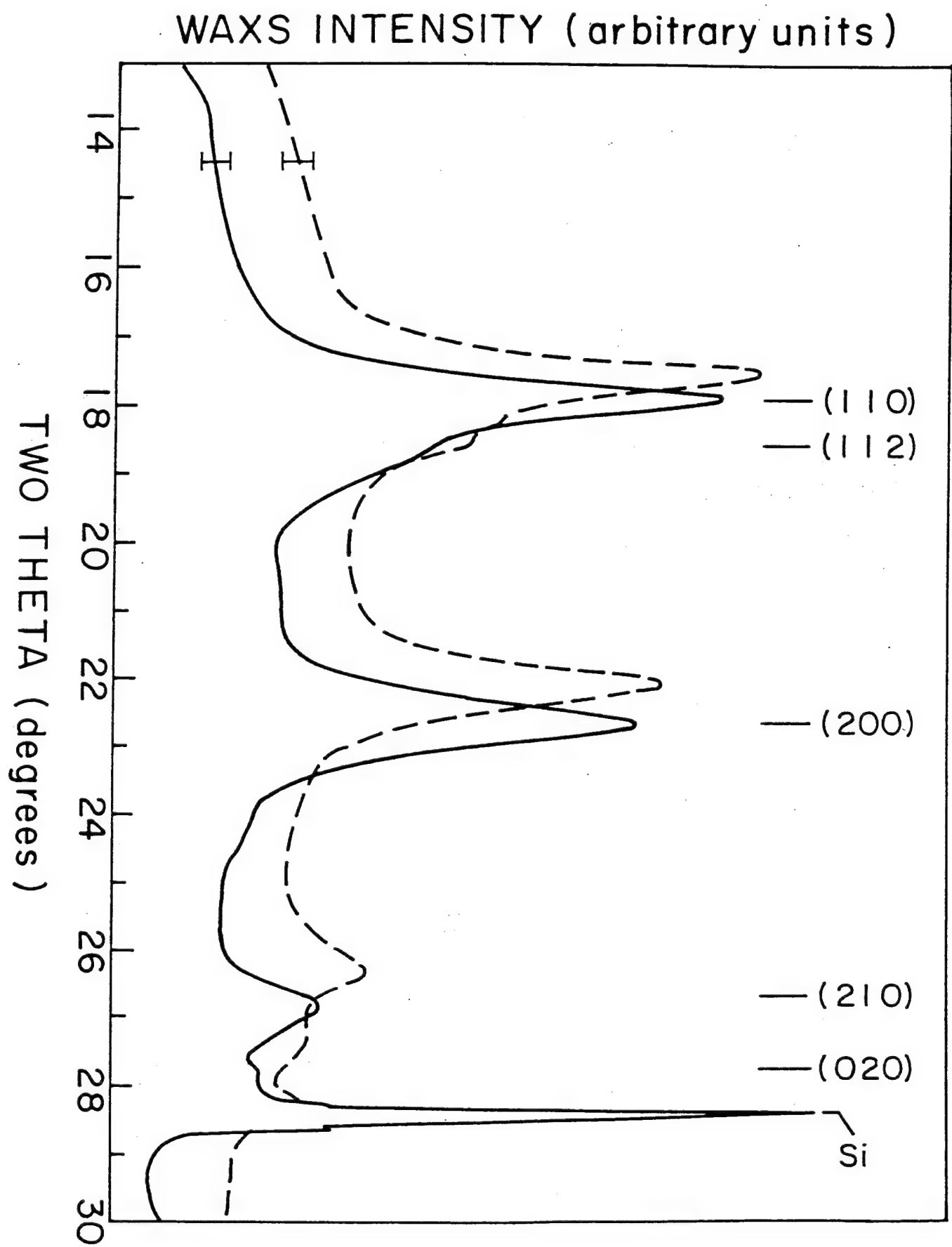


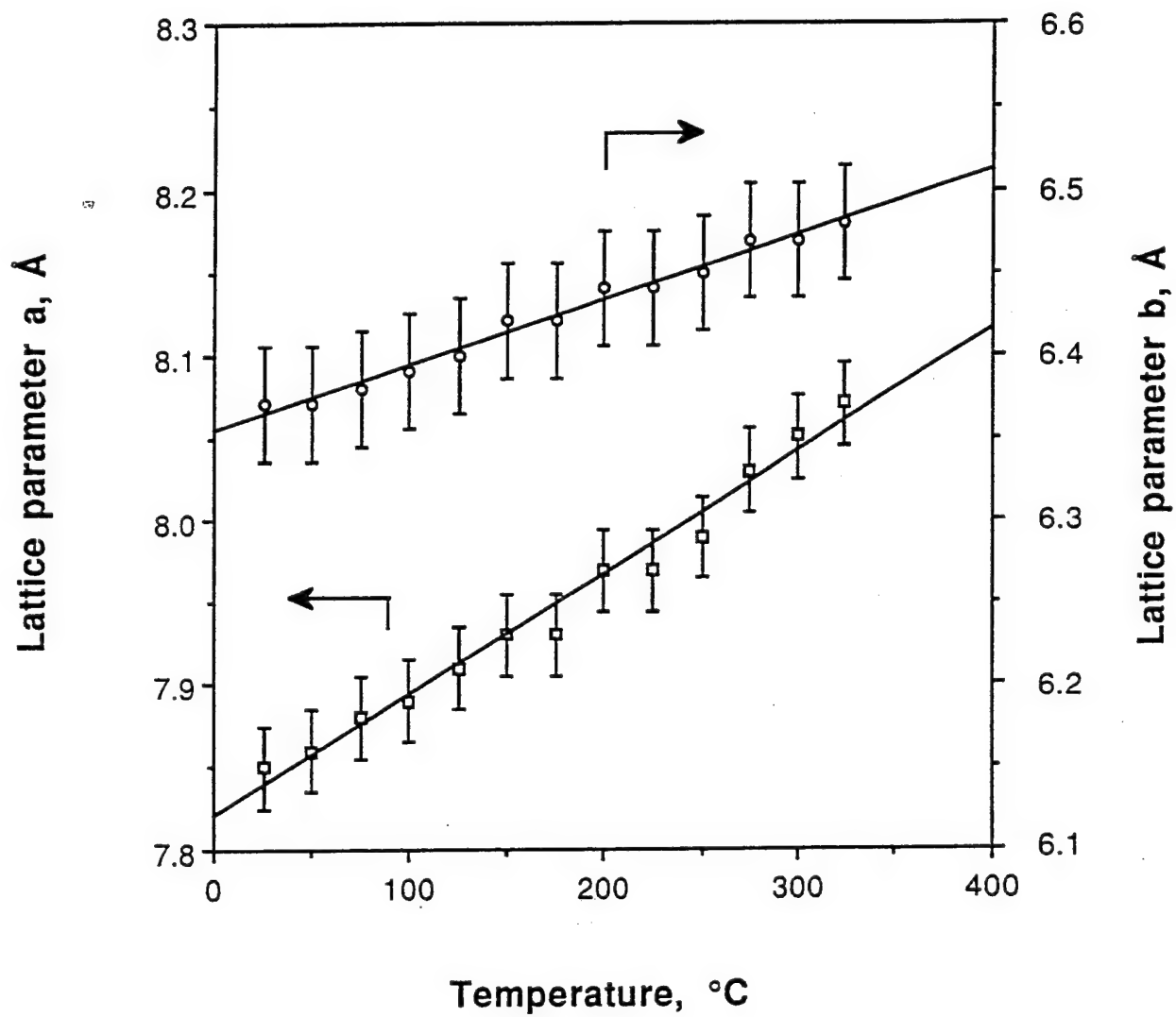


LARC-CPI

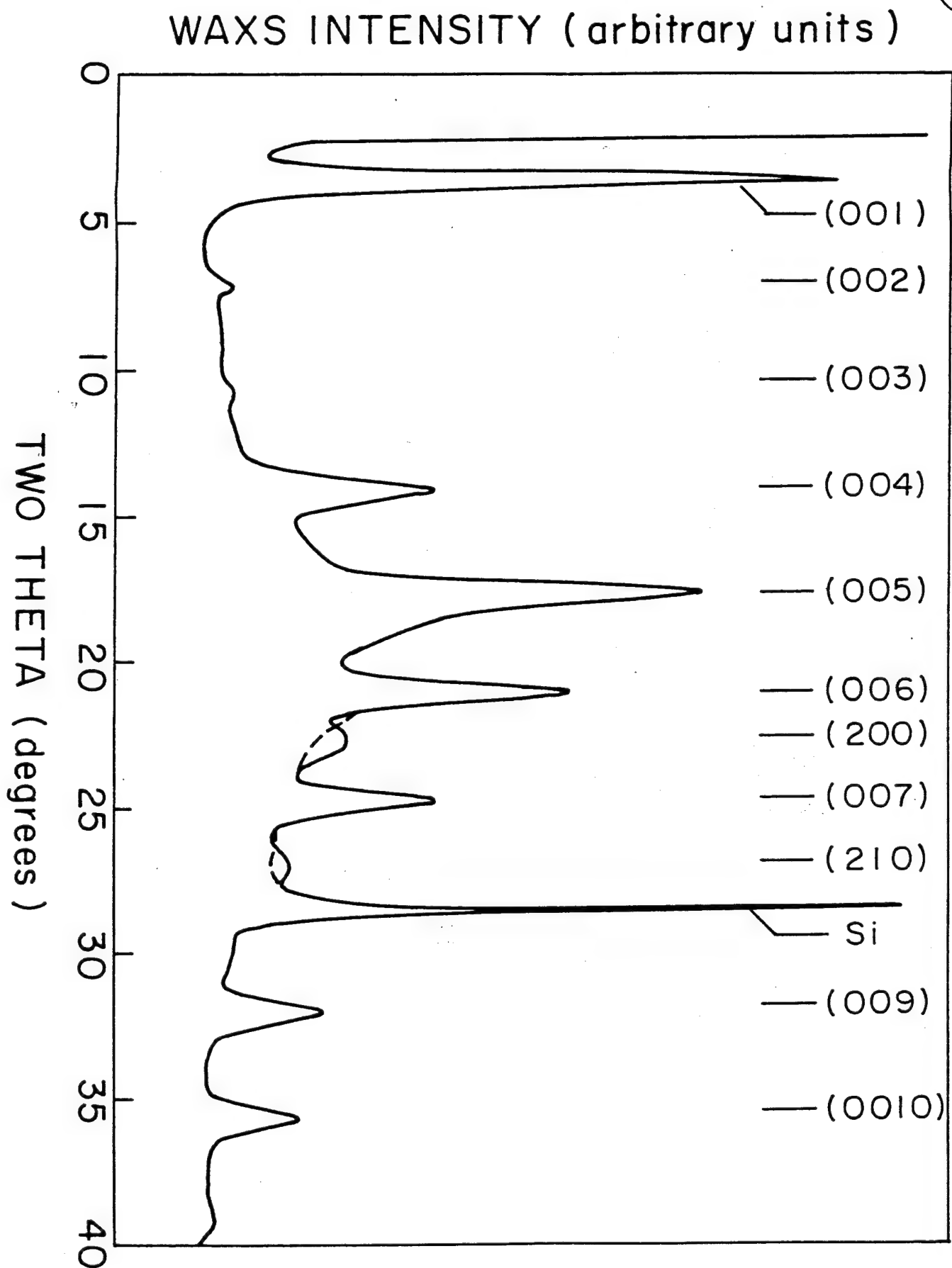
NEW-TPI



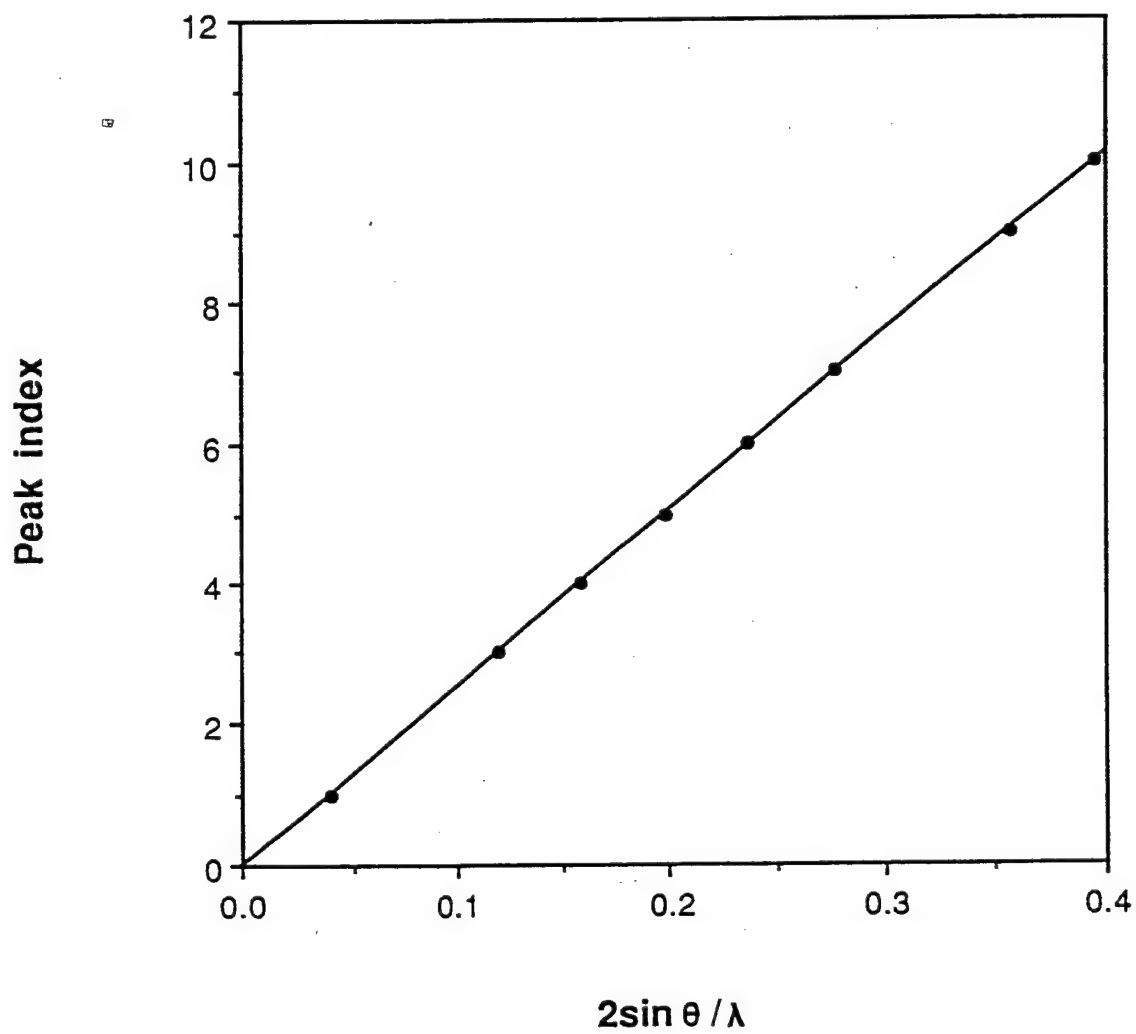




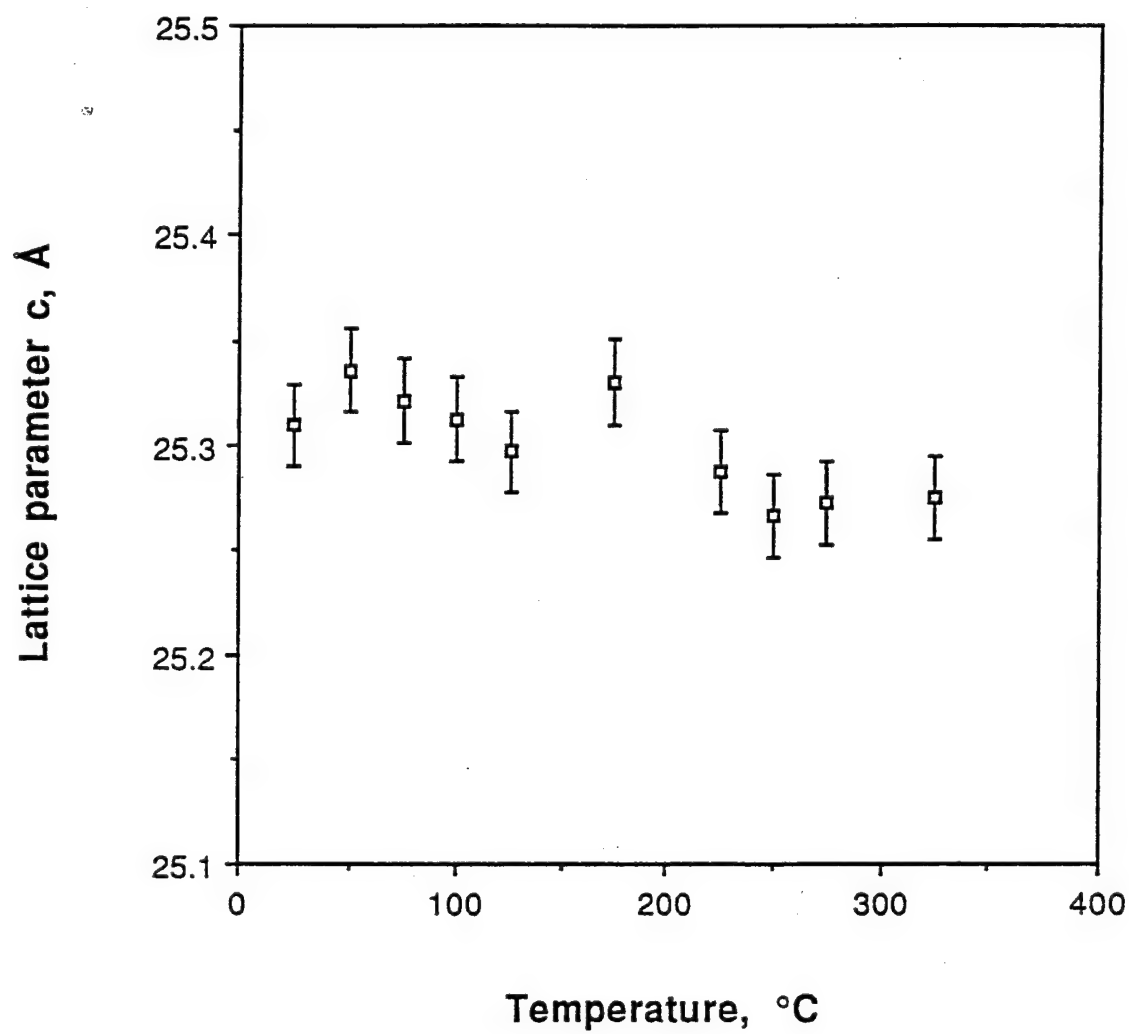
4

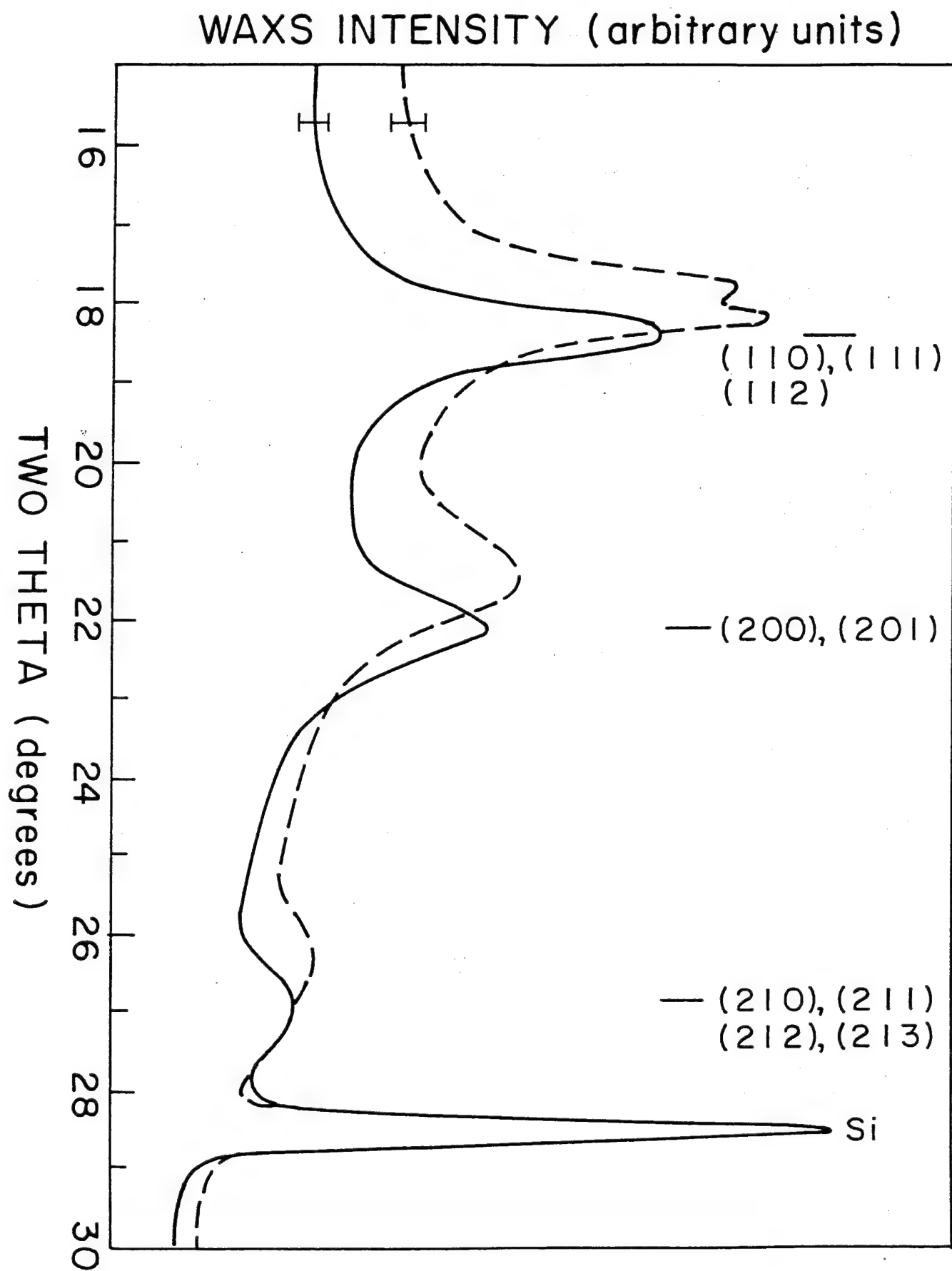


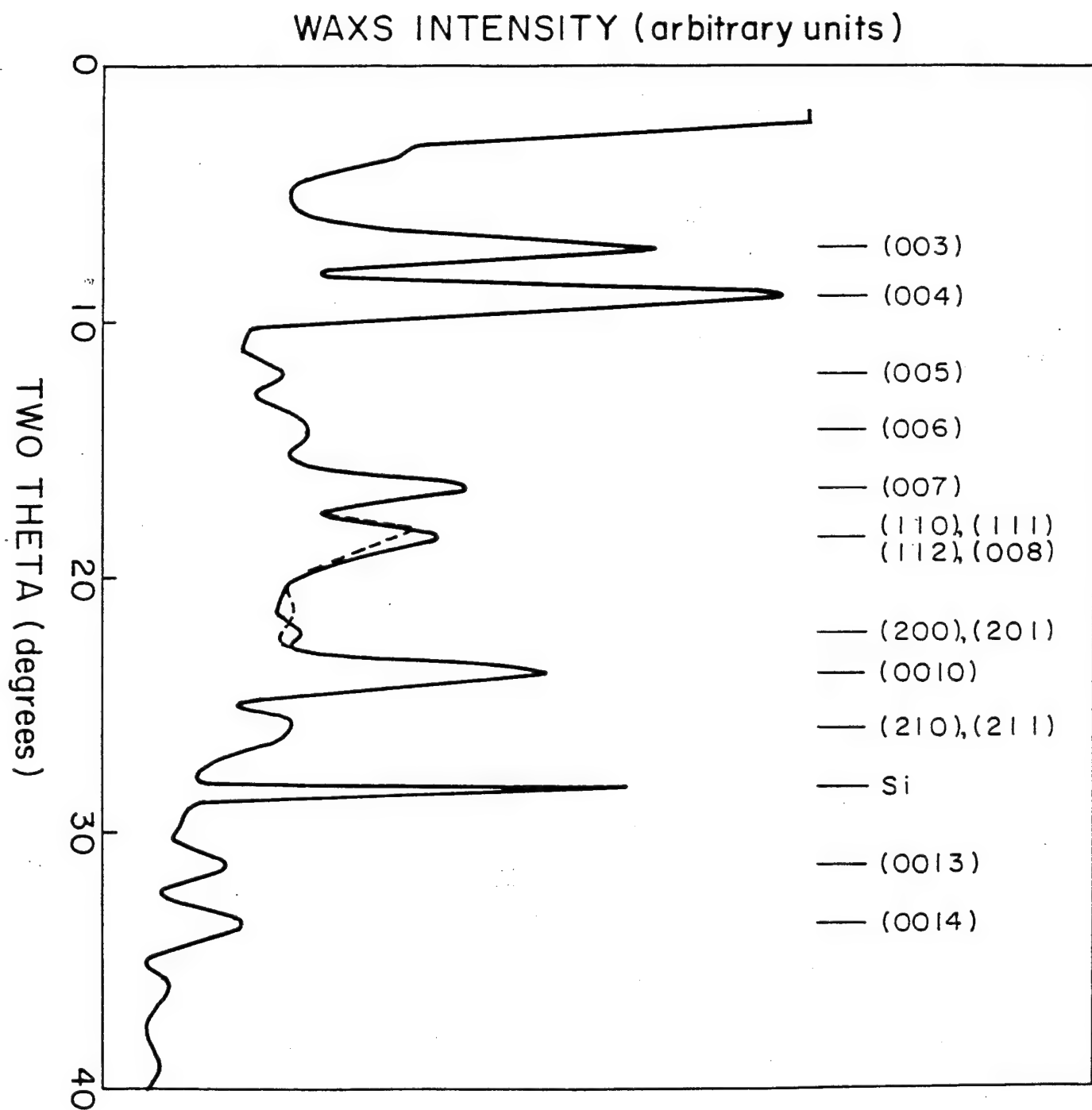
5a



5b

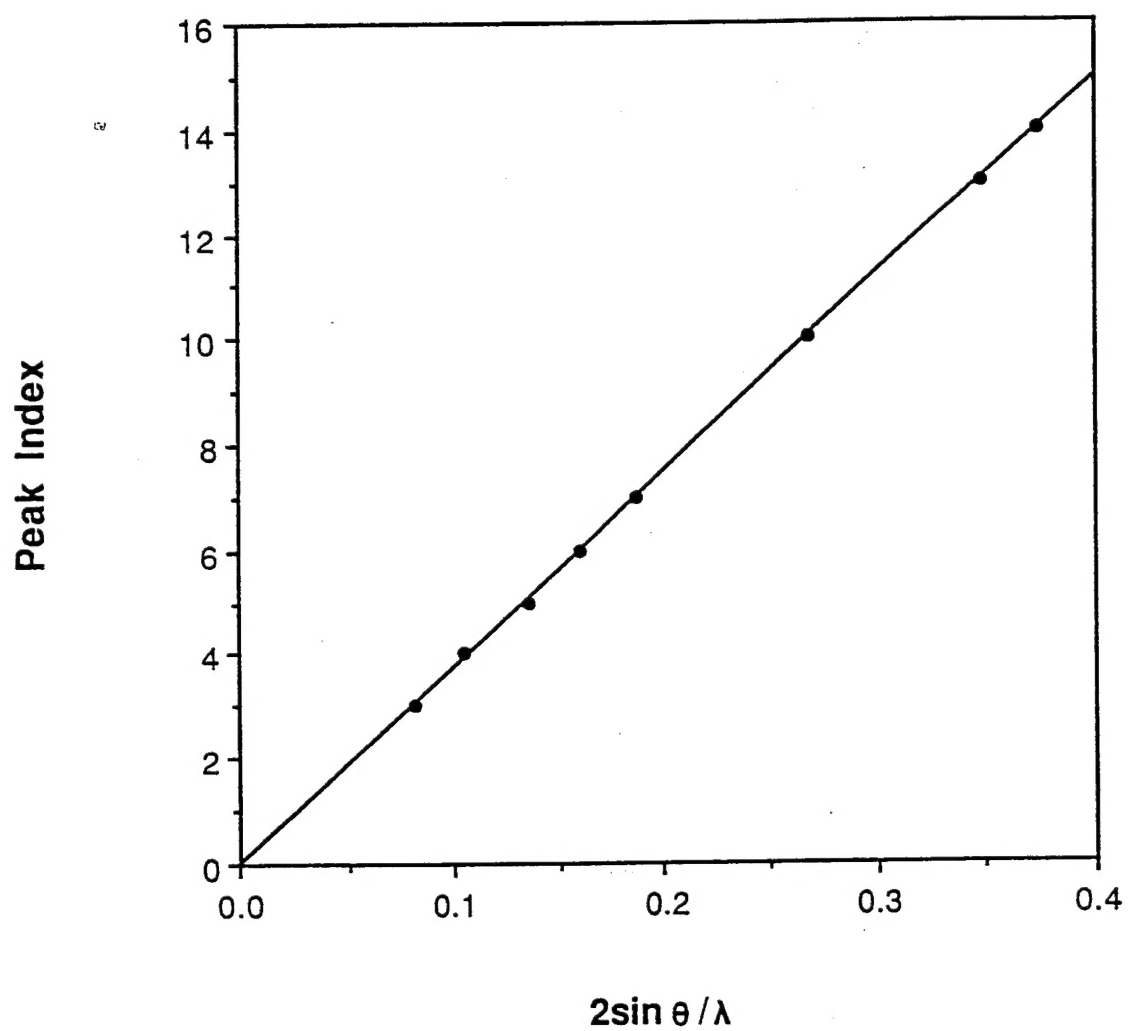


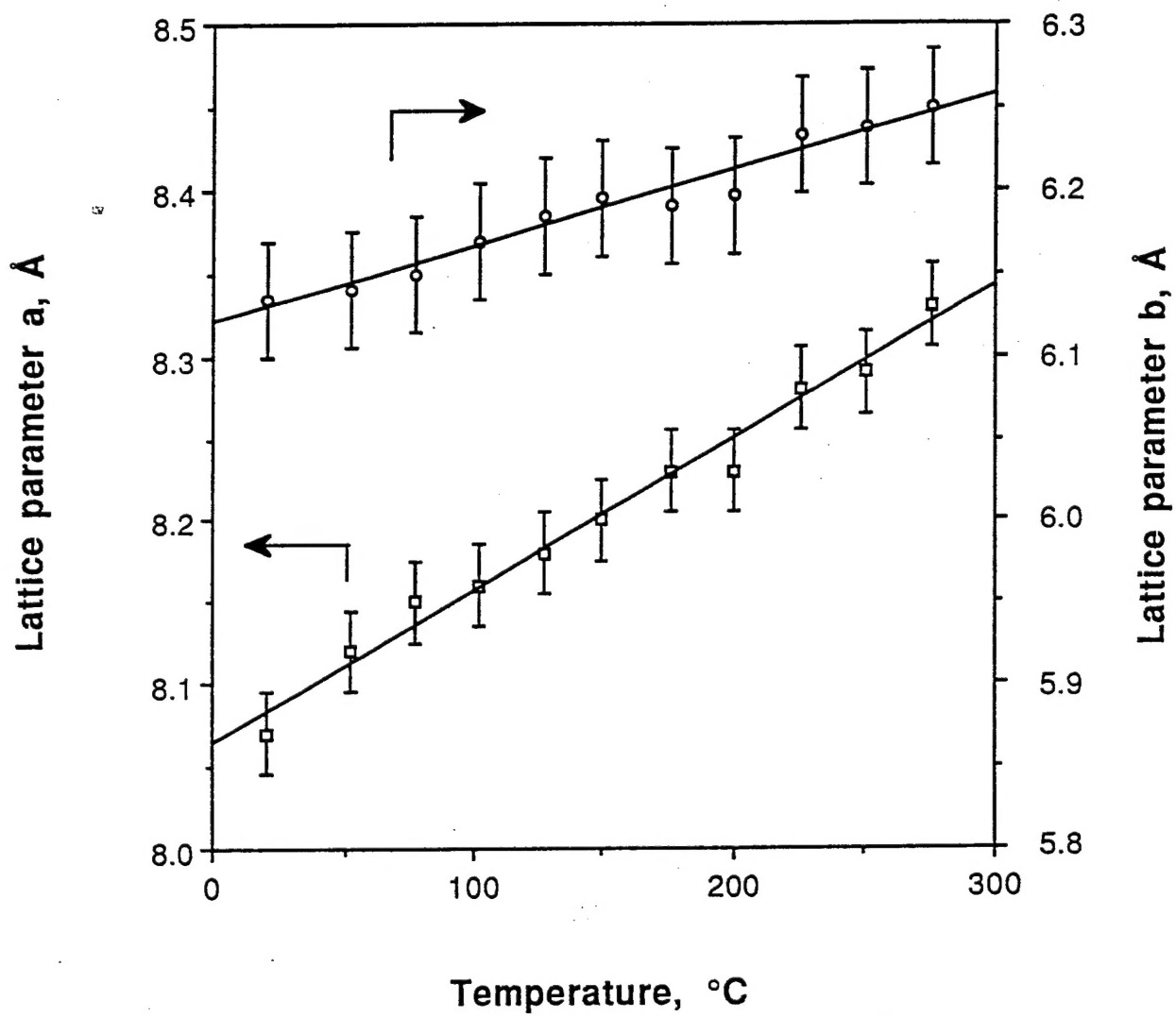






8





10a

